



TRANSIENT THERMAL PERFORMANCE OF A RADIALLY DILUTED AND CENTRALLY COOLED NUCLEAR FUEL CELL

F. Moukalled , R. Nuwayhid & I. Lakkis

To cite this article: F. Moukalled , R. Nuwayhid & I. Lakkis (1995) TRANSIENT THERMAL PERFORMANCE OF A RADIALLY DILUTED AND CENTRALLY COOLED NUCLEAR FUEL CELL, Numerical Heat Transfer, Part A: Applications, 28:6, 687-705, DOI: [10.1080/10407789508913769](https://doi.org/10.1080/10407789508913769)

To link to this article: <http://dx.doi.org/10.1080/10407789508913769>



Published online: 29 Oct 2007.



Submit your article to this journal [↗](#)



Article views: 13



View related articles [↗](#)

TRANSIENT THERMAL PERFORMANCE OF A RADIALLY DILUTED AND CENTRALLY COOLED NUCLEAR FUEL CELL

F. Moukalled, R. Nuwayhid, and I. Lakkis

*Faculty of Engineering and Architecture, Mechanical Engineering Department,
American University of Beirut, Beirut, Lebanon*

Steady and unsteady heat transfer in a radially diluted and centrally cooled nuclear fuel rod are investigated numerically. The nuclear fuel cell is radially diluted by the addition of a non-heat-generating material of high melting point, high specific heat, and high resistance to oxidation and ignition, with the intention of increasing its time delay before melting, when convection is totally lost. Results show a great reduction in the maximum wall temperature under steady operation and a substantial increase in the time delay under transient conditions, with its value increasing with increasing the amount of added diluent. Moreover, results indicate the presence of an optimum value of the ratio of inner to outer channel flow rates for which the maximum inner and outer wall temperatures are minimum. Finally, the distribution of the added diluent is shown to mildly affect the steady and unsteady performance of the reactor.

INTRODUCTION

One of the current major concerns in nuclear industry is safety and the cost entailed by its assurance. Following the explosion that blew apart the Soviet Union's Chernobyl Unit 4 nuclear reactor, which was mainly caused by human failure and poor operator judgment [1], attention was directed toward designing reactors that are inherently safe [1, 2]. The analysis undertaken here is along these lines and deals with studying the transient thermal performance of a newly suggested type of fuel rods, for use in the core of gas-cooled fast reactors (GCFR) that are capable, in case of loss of coolant, of absorbing their own generated heat for a longer period before melting.

Recently, Moukalled et al. [3] studied the thermal performance of radially diluted nuclear fuel cells and showed that the use of such rods results in a significant decrease in the maximum temperature during steady operation and a great increase in time delay before melting of the reactor core under unsteady conditions. The aim of this article is to extend the work reported in Ref. [3] to situations where the radially diluted rod is centrally cooled. This will force the heat generated by the fuel to be transported to the inner and outer coolants, creating

Received 24 February 1995; accepted 29 June 1995.

The financial support provided by the University Research Board of the American University of Beirut through grant 113040-48816 is gratefully acknowledged.

Address correspondence to Dr. F. Moukalled, Department of Mechanical Engineering, American University of Beirut, P.O. Box 11-0236, Beirut, Lebanon.

Numerical Heat Transfer, Part A, 28:687-705, 1995

Copyright © 1995 Taylor & Francis

1040-7782/95 \$10.00 + .00

687

within the fuel rods themselves to absorb this generated energy. Candidate diluents must have high specific heat, high density, high melting point, and be oxidation and ignition resistant. Ideally, it should not be a fuel material, although depleted UO_2 , as shown in this work, can be considered. The limiting factor should always be that the diluent must be in a sufficiently small amount so as to retain the fast character of the core [4, 5]. With this in mind, no attempt is made here to ascertain the neutronics of the diluted core design but merely an upper limit on the diluent-to-fuel ratio is imposed at random.

The problem is modeled and reduced to that of predicting the heat transfer characteristics of turbulent fluid flow around a longitudinally and radially conducting slender annular rod with internal heat generation. The heat produced in the "average" rod by the fission chain reaction is assumed to be radially independent with an axial cosine distribution [8]. The analysis is conducted for both steady and transient performance in case of a sudden and complete loss of coolant before shutting the reactor down. Initial conditions for the transient heat conduction problem in the fuel annulus are obtained from the steady state performance of the coolant-annulus and coolant-channel problems (Figure 1a).

The coupling between conduction in the fuel and convection in the fluid is accomplished by ensuring continuity of thermal conditions along the inner and outer walls of the annulus. These conditions are not known beforehand and have to be determined along with the solution to the problem. This adds to the complexity of the problem and necessitates the use of an iterative procedure in which the rod conduction and the fluid convection equations are successively solved until convergence. To model turbulence, the mixing length theory is used.

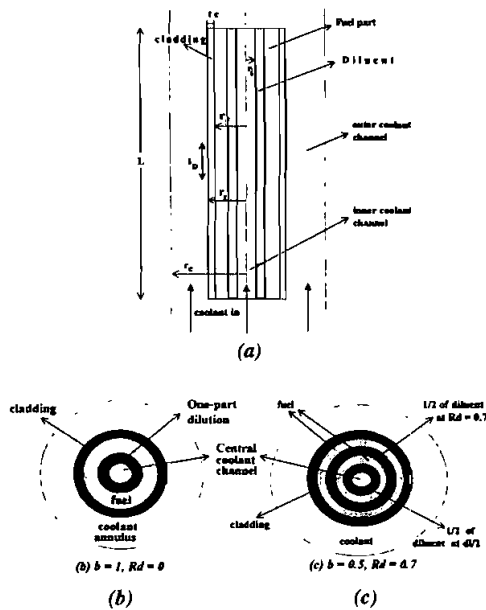


Figure 1. (a) Schematic of a radially diluted and centrally cooled fuel cell; (b) one-part dilution of a radially diluted and centrally cooled fuel cell; (c) two-part dilution of a radially diluted and centrally cooled fuel cell.

GOVERNING EQUATIONS AND BOUNDARY CONDITIONS

The physical situation under consideration, illustrated schematically in Figure 1a, represents the turbulent convection of a fluid around a longitudinally and radially conducting, slim annular rod with internal heat generation. Longitudinal diluent strips are added to the fuel annulus for various diameters of the inner coolant channel. The coolant is assumed to enter the annulus with uniform temperature and velocity profiles of values T_∞ and u_∞ , respectively. Moreover, the properties of the steady, two-dimensional axisymmetric flow are temperature dependent, and their expressions are displayed in Table 1a. The pressure of the coolant, chosen to be carbon dioxide, at the inlet to the annulus is assumed to be uniform and equal to 40 bars, a typical value of the pressure inside the pressurized vessel containing the reactor core [8].

In order to reduce the number of parameters involved, the following dimensionless variables are defined:

$$\begin{aligned} X &= \frac{x}{d_o} & \eta &= \frac{r}{d_o} & U &= \frac{u}{u_\infty} & V &= \frac{v}{u_\infty} \\ P &= \frac{p}{\rho u_\infty^2} & \theta &= \frac{T - T_\infty}{q_v d_o^2 / k_f} & t^* &= \frac{t}{d_o^2 / \alpha} \end{aligned} \quad (1)$$

Furthermore, axial diffusion in the fluid is neglected due to the high value of Péclet number in turbulent flow ($\gg 50$). With this assumption, the governing conservation equations may be expressed in parabolic forms and are detailed in the following sections.

Momentum Equation

The fluid momentum equation, in dimensionless form, may be written as

$$U \frac{\partial U}{\partial X} + V \frac{\partial U}{\partial \eta} = - \frac{dP}{dX} + \frac{1}{\text{Re}_\infty} \frac{1}{\eta} \frac{\partial}{\partial \eta} \left[\eta \left(1 + \frac{\mu_t}{\mu_l} \right) \frac{\partial U}{\partial \eta} \right] \quad (2)$$

where μ_l and μ_t are the laminar and turbulent viscosities, respectively.

Table 1a. Properties of coolant, fuel, cladding, and diluent (SI units)

	k	ρ	c_p	μ
Coolant				
Carbon dioxide (CO ₂)	$7.10238 \times 10^{-5} T$ -0.000615478	$21173.16/T$	$k/c_p = 3.3587 \times 10^{-5} \ln T$ -0.000176441	6.647×10^{-6} $+3.562 \times 10^{-8} T$
Fuel and diluent				
Uranium dioxide (UO ₂)	$7.536 - 0.00534T$ $+1.3 \times 10^{-6} T^2$	10,400	$228 + 0.274T - 0.00027T^2$ $+9.2 \times 10^{-8} T^3$	—
Cladding				
Stainless steel	$0.012T + 8.224$	7,900	$0.25T + 411.75$	—

The solution is obtained by solving two parabolic fluid flow problems in the outer and inner coolant channels and a conduction problem in the fuel rod. To solve the conservation of momentum equations governing the parabolic flow in the convection parts, the boundary conditions and the turbulent viscosity μ_t must be specified.

The boundary conditions for the coolant in the outer channel are

$$U = 1 \quad X = 0 \quad (3a)$$

$$\partial U / \partial \eta = 0 \quad \eta = D_c / 2 \quad (3b)$$

$$U = 0 \quad \eta = 0.5 \quad (3c)$$

whereas those for the inner channel are given by

$$U = 1 \quad X = 0 \quad (4a)$$

$$\partial U / \partial \eta = 0 \quad \eta = 0 \quad (4b)$$

$$U = 0 \quad \eta = D_i / 2 \quad (4c)$$

The turbulent viscosity μ_t is calculated using the mixing length model as described next.

Turbulence Model

The turbulence model employed here is Prandtl's mixing length model [9]. For simple annular and channel flows, such as those considered in this study, it has been shown to be adequate [3, 10]. In this model the turbulent viscosity μ_t is evaluated in terms of the mixing length and the local velocity gradient as

$$\mu_t = \rho l^2 \left| \frac{du}{dy} \right| \quad (5)$$

where l is the mixing length at a point situated at a distance y from the wall of the fuel rod ($y = r - d_o/2$ for the annulus and $y = d_i/2 - r$ for the inner channel) and is represented as the product of a Nikuradse-type mixing length l_n [11] and a Van Driest factor d_{VD} [12], i.e.,

$$l = l_n d_{VD} \quad (6)$$

For turbulent annular flow between inner diameter d_o and outer diameter d_c , l_n and d_{VD} are given by

$$\frac{l_n}{(d_c - d_o)/2} = 0.14 - 0.08 \left(1 - \frac{y}{(d_c - d_o)/2} \right)^2 - 0.06 \left(1 - \frac{y}{(d_c - d_o)/2} \right)^4 \quad (7)$$

$$d_{VD} = 1 - \exp \left[- \left(\frac{\rho y}{26 \mu_1} \right) \sqrt{\frac{\tau_w}{\rho}} \right] \quad (8)$$

where τ_w is the local shear stress on the pipe wall. The expression $(d_c - d_o)$ is replaced by d_i for the case of inner channel flow. By combining Eqs. (6)–(8), the mixing length l and, consequently, μ_t (Eq. (5)) are completely specified.

Energy Equations

The conservation of energy equation for the axisymmetric parabolic flow problems, in dimensionless form, can be written as

$$U \frac{\partial \theta}{\partial X} + V \frac{\partial \theta}{\partial \eta} = \frac{1}{\text{Pe}} \frac{1}{\eta} \frac{\partial}{\partial \eta} \left[\eta \left(1 + \frac{\epsilon_H}{\alpha} \right) \frac{\partial \theta}{\partial \eta} \right] \quad (9)$$

The boundary conditions used to solve the above equation in the outer channel are

$$\left(\frac{\partial \theta}{\partial \eta} \right)_{w(f)} = K \left(\frac{\partial \theta}{\partial \eta} \right)_{w(s)} \quad \eta = 0.5 \quad (10a)$$

$$\frac{\partial \theta}{\partial \eta} = 0 \quad \eta = D_c/2 \quad (10b)$$

$$\theta = 0 \quad X = 0 \quad (10c)$$

whereas for the inner channel the applied boundary conditions are given by

$$\left(\frac{\partial \theta}{\partial \eta} \right)_{w(f)} = K \left(\frac{\partial \theta}{\partial \eta} \right)_{w(s)} \quad \eta = D_i/2 \quad (11a)$$

$$\frac{\partial \theta}{\partial \eta} = 0 \quad \eta = 0 \quad (11b)$$

$$\theta = 0 \quad X = 0 \quad (11c)$$

The dimensionless energy equation for the steady and unsteady heat conduction problems in the fuel rod is

$$\frac{\partial \theta}{\partial t^*} = \frac{1}{\eta} \frac{\partial}{\partial \eta} \left(K \eta \frac{\partial \theta}{\partial \eta} \right) + \frac{\partial}{\partial X} \left(K \frac{\partial \theta}{\partial X} \right) + j \frac{\pi}{2} \cos \left[\pi \left(\frac{X}{L_r} - \frac{1}{2} \right) \right] \quad (12)$$

where K is the solid to fluid thermal conductivity ratio, $j = 1$ in the fuel, and $j = 0$ in the cladding and diluent.

The boundary conditions for the conduction energy equation are

$$\frac{\partial \theta}{\partial X} = 0 \quad X = 0 \quad X = L_r \quad (13a)$$

$$\theta = \theta_{w(in)}(X) \quad \eta = D_i/2 \quad (13b)$$

for steady state performance,

$$\theta = \theta_{w(out)}(X) \quad \eta = 0.5 \quad (13c)$$

for steady state performance,

$$\frac{\partial \theta}{\partial \eta} = 0 \quad \eta = D_i/2 \quad (13d)$$

for transient performance, and

$$\frac{\partial \theta}{\partial \eta} = 0 \quad \eta = 0.5 \quad (13e)$$

for transient performance, where $\theta_{w(in)}(X)$ and $\theta_{w(out)}(X)$ are the temperatures along the inner and outer walls of the fuel rod, respectively, which are not known a priori but are determined from solving the convection energy equations for the inner and outer coolant channels. Moreover, the parameters $\theta_w(X)$ and $(\partial \theta / \partial \eta)_w$ provide the coupling between the convection and conduction problems. Furthermore, it should be pointed out here that under transient conditions and due to the lack of any better information, the walls of the fuel annulus in contact with the coolant during steady performance are assumed to be insulated (Eqs. (13d) and (13c)). Thus results generated in this article simulate the worst probable situation that could arise during an accident. Therefore any improvement in thermal performance of the fuel rod is expected to further magnify if this condition is relaxed.

FUEL ROD PARAMETERS AND CONFIGURATIONS

The number of parameters involved in the problem is large, and thus, analyzing the effect of varying each of these parameters is computationally not feasible due to the large number of cases to be considered. Consequently, the effect of varying selected parameters is only studied, and the remaining parameters (Table 1b) are fixed throughout the analysis. The streamwise heat source distribution in the fuel is calculated from $q(x) = q_{max} \cos \pi(X/L' - 1/2)$, where $q_{max} = (\pi/2)q_{ave}$ and $L' = L + \Delta$ is the extrapolated fuel rod length, which is obtained from the (nonzero) value of the heat flux generated at the extremities of the fuel rod (i.e., $X = 0$ and L_r). To further elaborate, the extrapolated length arises in

Table 1b. Parameters kept fixed throughout the analysis

Parameter	Dimensional value
Coolant annulus sectional area	0.0000676648 m ²
Cladding thickness	0.00035 m
Fuel cross-sectional area	0.0000384845 m ²
Fuel length	1.5 m
Energy produced in the fuel	25189 W
Coolant inlet conditions	
Temperature	525 K
Axial velocity component	30 m/s
Pressure	40 bars

connection with the so-called free surface boundary condition: the neutron flux is required to vanish just beyond the physical length due to leakage of neutrons from the rod. A simplistic and approximate relation for Δ may be written as

$$\Delta = \frac{\delta}{d_o} \quad \delta \cong \frac{0.71}{\Sigma_s[1 - (0.67/M)]} \quad (14)$$

where Σ_s is the fuel macroscopic scattering neutron cross section and M is the fuel molecular weight. For large fast cores, δ is usually in the range of 5–10 cm.

Dilution is accomplished by one of the following two ways: one-part dilution, and two-part dilution. In both cases the diluent extends axially all over the fuel rod. One-part dilution, shown in Figure 1b, places the diluent directly around the inner coolant channel (i.e., at $r = d_i/2$). Two-part dilution (Figure 1c) is made by having half the diluent placed at $r = d_i/2$ and the other half at a distance of $R_d = 0.7$.

SOLUTION PROCEDURE AND COMPUTATIONAL DETAILS

For the convection problems, the fluid momentum and energy equations, Eqs. (2) and (9), are solved numerically using the parabolic calculation procedure of Patankar and Spalding [13]. This is a fully implicit, marching type solution procedure, proceeding from the inlet location ($X = 0$) to the exit of the annulus ($X = L_r$). The heat conduction problem in the fuel rod, Eq. (12), is solved by the elliptic finite volume method described by Patankar [14].

The conjugate conduction-convection coupling is solved via an iterative approach in which the momentum and energy equations for the fluid and the energy equation for the fuel annulus are solved consecutively. To start the first iteration, the fuel energy equation, Eq. (12), is solved by imposing guessed values for $\theta_{w(in)}(X)$ and $\theta_{w(out)}(X)$ as the boundary conditions needed in Eqs. (13b) and (13c), respectively. The solution obtained is fed into the fluid energy equation, Eq. (9), via the terms $(\partial\theta/\partial\eta)_{\eta=D_i/2}$ (for the inner channel) and $(\partial\theta/\partial\eta)_{\eta=0.5}$ (for the outer channel), which is solved for the inner and then the outer channel (or vice versa) to obtain updated values for $\theta_{w(in)}(X)$ and $\theta_{w(out)}(X)$, respectively. The updated $\theta_{w(in)}(X)$ and $\theta_{w(out)}(X)$ are used to initiate the second iteration, and the

fuel rod energy equation is solved again. This procedure is continued until convergence to at least four significant figures is reached.

The computational task is fairly demanding in terms of both computer time and computer storage. This is mainly due to the consecutive iterative scheme used to resolve the conduction-convection coupling. The flow computations in the outer and inner channels were performed with 175 grid points scanning the annulus cross sections ($0 \leq \eta \leq D_i/2$ and $0.5 \leq \eta \leq D_c/2$) and clustering near the rod walls. In the axial direction a uniform step size of value 10^{-3} was used for all tested cases, giving a total number of 1500 grid points in the streamwise direction. The 1500×175 mesh system was found to be adequate for producing grid-independent results. For the solution of the fuel rod conduction equation for both steady and unsteady situations, the mesh consisted of 71 grid points in the axial direction and 54 grid points in the radial direction. When transferring data from the steady conduction problem to the convection problems, linear interpolation was employed. The step size in the flow problems was sometimes modified to allow for the conduction control volume radial faces to be identical to streamwise positions in the flow solution, so that the transfer of information from the flow problems to the conduction problem is easy and direct.

RESULTS AND DISCUSSION

The main parameters of interest in this study are the ratio of the volume of added diluent to total fuel rod volume (a), the location of the added diluent (R_d) and its percentage (b), and the ratio of the outer to inner coolant mass flow rates (RC). Parameter values considered are four different values of a ($a = 0.1, 0.2, 0.3$, and 0.5), two values of R_d and b ($b = 1$ and $R_d = 0$; $b = 0.5$ and $R_d = 0.7$), and four values for RC (RC = 0.5, 1, 2, and 3). The purpose of varying a is to investigate the effectiveness of the heat sink, represented by the diluent, as compared with the heat source represented by the fuel with respect to temperature distribution in the fuel annulus. The second parameter aims at anticipating the effects of redistributing the added diluent. Two possible distributions are investigated; the first locates all the diluent as an inner cladding around the central coolant channel ($b = 1$ and $R_d = 0$), whereas the second locates half the diluent around the central channel and the other half at a radius that is equal to 0.7 times the outer fuel radius ($b = 0.5$ and $R_d = 0.7$). Finally, the third parameter RC predicts the effects of varying the inner and outer flow rates on the maximum inner and outer wall temperatures of the fuel rod. Only one diluent material (natural and totally depleted UO_2) was tested due to the mild influence of the material used on the thermal performance of the fuel rod [3]. However, since the diluent (or part of it in two-part dilution) will contact the coolant in the central channel, it would be definitely preferable to have a diluent that is a nonfuel such as Al_2O_3 , B_4C . . . , but this is not of concern in this article.

In order to reveal the influence on heat transfer of the various parameters involved, results are presented in terms of streamwise variations of wall temperature, maximum wall temperature, exit bulk temperature, average Nusselt number, and heat flux. Finally, using the steady temperature distribution in the fuel rod as

the initial condition, transient behavior is investigated for the respective cases, and transient performance curves are generated.

Due to unavailability of any experimental data related to the problem at hand, results are validated by comparing numerical values of steady state conduction obtained in the original rod with results generated analytically using various empirical turbulence models. The numerical results, not presented here for compactness, are found to fall in the range of results generated by the empirical models. For further details, the reader is referred to the previous work reported by the authors [3].

Steady Conjugate Heat Transfer Results

Wall heat flux. The total heat generated by the fuel (Q) is partly conducted to the coolant in the annulus across the outer wall (q_{out}) and the rest to the coolant in the channel across the inner wall (q_{in}) such that

$$Q = q_{out} + q_{in} = \text{const} \quad (15)$$

However, q_{out}/q_{in} depends on the ratio of the outer to inner thermal resistances to radial heat flow, which is a function of the outer to inner wall areas. Consequently, the division of the total energy generated between the outer and inner coolants is strongly dependent on the outer to inner channel diameter ratio d_o/d_i . This dependence is clearly shown in Figure 2a, where the variation of q_{out}/q_{in} is plotted as a function of RC or $(d_o/d_i)^2$ for $a = 0.3$. As depicted, the amount of heat conducted across the outer wall increases with increasing values of d_o/d_i (or RC) due to an increase in the outer coolant mass flow rate, which decreases the outer coolant bulk temperature and creates higher outer radial temperature gradients.

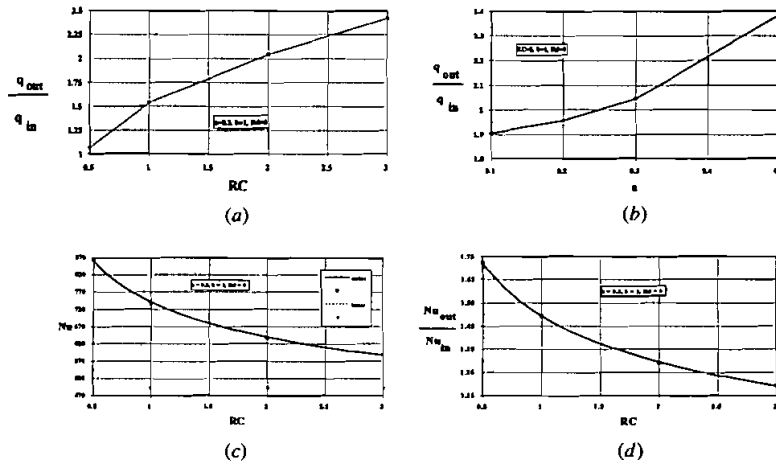


Figure 2. (a) Variation of the outer to inner wall heat flux ratio with RC. (b) Variation of the outer to inner wall heat flux ratio with a . Variation of the average (c) inner and outer Nusselt numbers and (d) their ratio with RC.

The decrease in the inner wall heat flux with increasing values of a is clearly seen in Figure 2b and is due to the increase and decrease in the outer rod diameter and the outer coolant bulk temperature, respectively.

Nusselt numbers. The local and average Nusselt numbers are defined as

$$\text{Nu} = \frac{hd_o}{k_f} \quad \text{Nu}_{\text{ave}} = \frac{h_{\text{ave}}d_o}{k_{f\text{ave}}} \quad (16)$$

The variation of the average outer and inner Nusselt numbers with RC and their ratio are presented, for $a = 0.3$, in Figures 2c and 2d, respectively. The average values of Nu_{out} are seen to decrease as RC increases, whereas the average values of Nu_{in} are more or less constant (Figure 2c). As RC increases, the outer flow area increases and the outer diameter of the fuel rod decreases. Consequently, the rate of increase in velocity away from the wall is lower for higher values of RC, which indicates lower values of the heat transfer coefficient (i.e., the average velocity is constant, and the flow area increases with increasing RC values). The variation in k_f values with temperature is comparatively small, so that the combined effect of h , d_o , and k_f is a net decrease in the average values of Nu_{out} . The slight variation in the values of Nu_{in} may be explained by noting that the inner Nusselt number is also based on the outer diameter ($\text{Nu}_{\text{in}} = h_{\text{in}}d_o/k_f$), which decreases as RC increases, so that it offsets the increase in the heat transfer coefficient, keeping Nu_{in} almost constant. Since Nu_{out} is decreasing and Nu_{in} is nearly constant, their ratio should decrease as RC increases, as shown in Figure 2d.

Coolant bulk temperatures. The coolant bulk temperature is defined as

$$T_{\text{bulk}} = \frac{\int_{r_1}^{r_2} \rho u(2\pi r dr) c_p T}{\int_{r_1}^{r_2} \rho u(2\pi r dr) c_p} \quad (17)$$

where $r_1 = 0$, $r_2 = d_i/2$ for the inner channel, and $r_1 = d_o/2$, $r_2 = d_c/2$ for the outer channel. Since k_f varies slightly with temperature (Table 1a), Eq. (1) shows that variations in the dimensionless bulk temperature reflect nearly the same variations in the dimensional bulk temperature. Moreover, the bulk temperature at a certain streamwise location is related to the energy conducted across the wall up to that location according to the following relation:

$$q_{\text{out}}(0 \rightarrow x) = m_{\text{out}} c_{p(f)} [T_{\text{bulk}}(x) - T_{\text{in}}] \quad (18)$$

At constant RC values, neglecting the slight dependence of $c_{p(f)}$ on temperature, Eq. (18) shows that for higher values of q_{out} anticipated with higher a , the outer exit T_{bulk} should experience higher values (Figure 3a). Consequently, the exit T_{bulk} associated with the inner coolant channel should decrease with increasing values of a (Figure 3a) due to the lower energy conducted radially inward. Furthermore, the ratio of outer to inner exit T_{bulk} for various dilutions varies approximately between 0.9 and 1.3 (Figure 3b), with a value of 0.98 obtained for an a value of 0.2 and resulting in nearly equal inner and outer exit T_{bulk} .

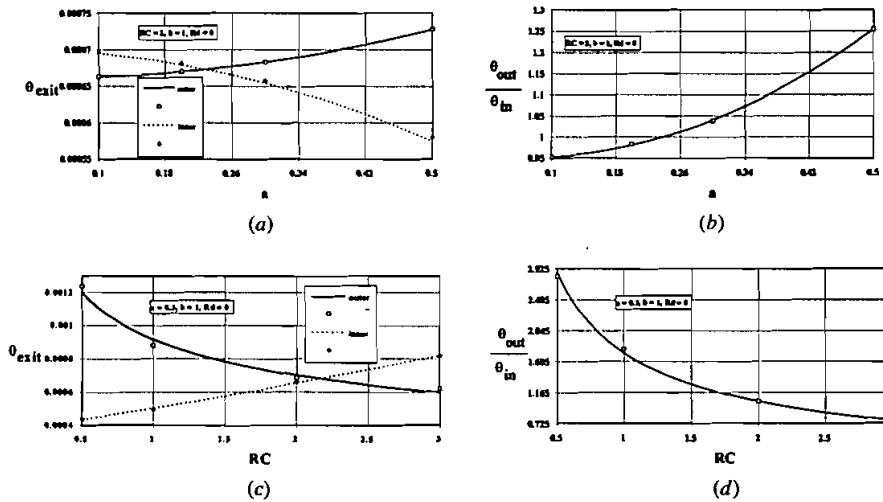


Figure 3. Variation of (a, c) outer and inner exit coolant bulk temperatures and (b, d) their ratio with a and RC.

At constant a values, a major rise in the outer exit T_{bulk} occurs as RC decreases. This is expected because decreasing RC results in lower outer coolant mass flow rate and a decrease in the heat conducted radially outward. Therefore the T_{bulk} should increase because a simple calculation (using Eq. (18)) reveals that q_{out} decreases at a lower rate than the outer coolant mass flow rate. This effect on T_{bulk} results in major changes in its value, as depicted in Figure 3c. On the other hand, lower values of RC are associated with lower exit T_{bulk} in the inner channel. This is further revealed in Figure 3d, where the variations of the outer to inner exit T_{bulk} are presented. Furthermore, it can be inferred from the figures that a value of RC = 2.2 results in equal outer and inner exit T_{bulk} .

Wall temperatures. The streamwise variation of wall temperatures (Figure 4) shows the same general behavior of increasing from zero at the inlet to a maximum somewhere beyond the center, and then decreasing all the way to the exit. Even though the heat source has a cosine distribution that maximizes at the middle of the fuel annulus, the maximum wall temperature is shifted toward the exit due to the interaction of the heat source with the convective coolant of steadily increasing T_{bulk} .

In Figure 4a the axial variation of θ_{in} with a is depicted. Increasing a results in lower heat conducted radially inward and lower inner T_{bulk} . Therefore, since q_{in} should satisfy the following equation,

$$q_{in} = k_f A_w \left(\frac{dT}{dr} \right)_w \quad (19)$$

and since the fluid-wall contact area is constant (RC = 2) and variations in k_f are comparatively small, the radial gradient of temperature at the wall should de-

crease, leading to lower inner wall temperature levels. On the other hand, increasing a results in a larger outer coolant-fuel contact area, higher heat conducted radially outward, higher fluid temperatures, and lower radial thermal resistance in the outward direction, so that the net effect is an increase in the outer wall temperatures, as shown in Figure 4*b*. Moreover, for $RC = 2$ the value of a that yields equal outer and inner maximum wall temperatures is ~ 0.41 (Figure 4*c*). In addition, Figures 4*c* and 4*d* show that, as a increases, the rate of decrease in the maximum inner wall temperature is higher than the increase in the outer wall temperature. This is to our advantage and is due to the increase in the outer area

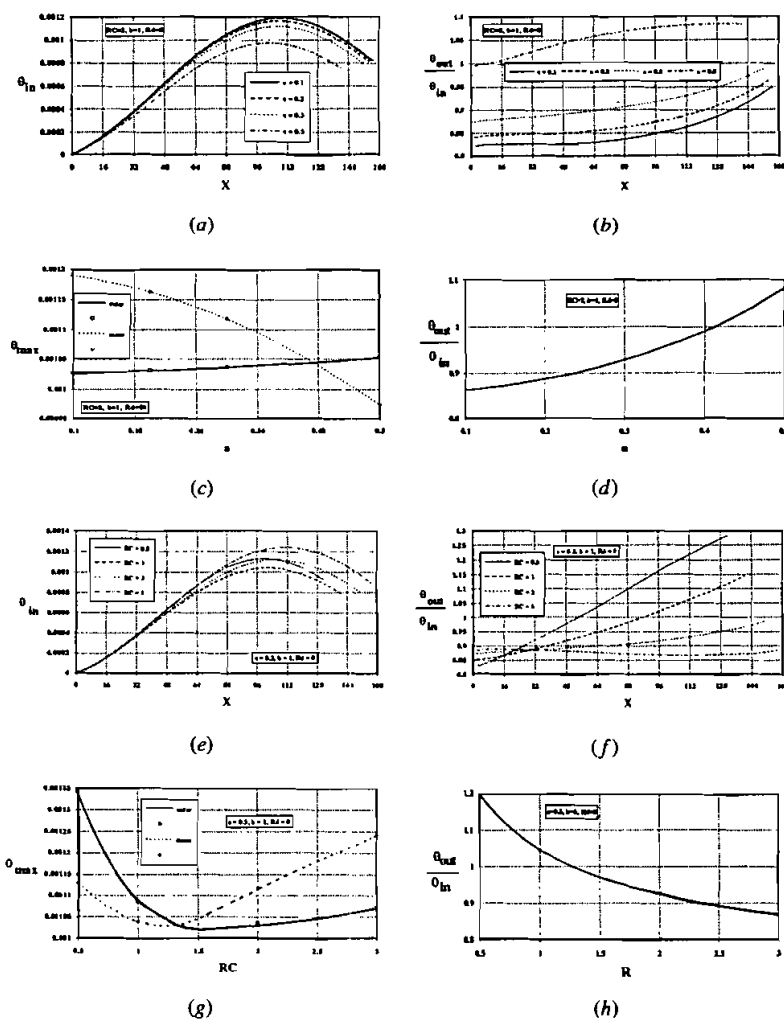


Figure 4. Streamwise variation of (a, e) inner wall temperature and (b, f) the ratio of outer to inner wall temperatures for various values of a and RC . Variation of (c, g) maximum outer and inner wall temperatures and (d, h) their ratio with a and RC .

of the fuel rod (the inner area is constant), which contributes to the outer heat flux (Eq. (18)), requiring less increase in the outer wall temperature for a given q_{out} . As shown in Figure 4c, the decrease in the maximum inner wall temperature reaches about 20% as a varies from 0.1 to 0.5.

Increasing RC results in a decrease in the heat conducted across the inner wall, as discussed earlier. Moreover, it produces a reduction in the coolant channel diameters such that the reduction in the inner diameter is greater than that in the outer diameter, resulting in a net increase in the rod annulus thickness. The interaction of the decreasing heat conducted across the inner wall, together with the variation of the thermal resistance to radial conduction associated with the increasing rod annulus thickness, results in the streamwise distributions of the inner wall temperature depicted in Figure 4e.

The streamwise variations of the outer to inner wall temperature ratio (θ_{out}/θ_{in}) for various values of RC are presented in Figure 4f. It may be noted that for low RC values, the outer wall temperature is very high compared with the inner wall temperature due to the small coolant mass flow rate associated with the outer channel. As RC increases, a higher coolant mass flow rate across the outer channel is anticipated at the expense of that in the inner channel, which results in lower outer wall temperatures. Once the optimal outer to inner coolant flow area ratio is reached, increasing RC further results in a reverse effect on the outer wall temperature. This is further revealed in Figure 4g, where the maximum inner and outer wall temperatures are seen to decrease with increasing RC until reaching a minimum, and then to rise again. Such behavior implies the presence of an optimum RC value (between 1 and 2, Figures 4g and 4h), for which the maximum wall temperatures are minimum.

It should be mentioned here that the design temperature is the maximum outer wall temperature associated with the cladding surface. As will be seen below, even though the maximum wall temperatures are lower than the maximum fuel temperatures, they are closer to their limiting values. Furthermore, the limiting value of the inner wall temperature is the melting point of the UO_2 diluent, which is much higher than that of the cladding (stainless steel), so that attention should be focused on the maximum outer wall temperature. However, if stainless steel is to be used as a diluent instead of uranium dioxide, then equality of the maximum outer and inner wall temperatures will yield optimum performance of the fuel rod because failure will occur whenever any of them reaches the melting point of stainless steel. Moreover, the maximum allowable temperature is actually the fault temperature, which is lower than the melting temperature and beyond which the material loses its strength. However, in this work, the melting point is assumed to be the limiting temperature. Furthermore, results generated here indicate that optimum performance is associated with $RC = 2$, where the maximum outer wall temperature reaches a minimum of 0.001075, which is about 54% of that corresponding to the original rod, and about 86% of the value reported in Ref. [3] for the case where there is no central channel and maximum radial dilution ($RC = \infty$, $a = 0.7$). The maximum inner wall temperature corresponding to $RC_{optimal}$ is nearly 0.00112.

At this point it should be clarified that adding a diluent poses a problem regarding the "fast" characteristic of the reactor, since such a diluent acts as a

moderator that slows down the neutrons. Thus, if diluent is added, a smaller amount is preferable to a larger one even though higher wall temperatures are anticipated. As demonstrated here, introducing a central channel in the fuel rod produces significant improvements in its steady state performance as compared with the original fuel rod configuration and shows an even better performance than all diluted rods discussed in Ref. [3] for less diluent addition. Therefore this configuration yields very promising results regarding the required improvements in thermal performance, without appreciably affecting the "fast" mode or characteristic of the reactor core.

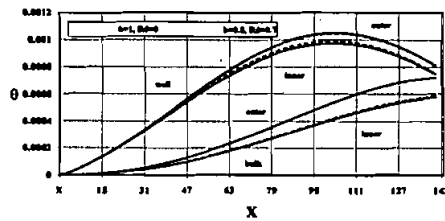
Finally, redistributing the diluent using the two-part dilution practice proves to have very mild influence on the thermal performance of the fuel rod. As shown in Figure 5a, two-part dilution results in a slight decrease in the bulk and wall temperatures along the outer channel, faced by an equivalent increase along the inner channel.

Unsteady Conduction Heat Transfer Results

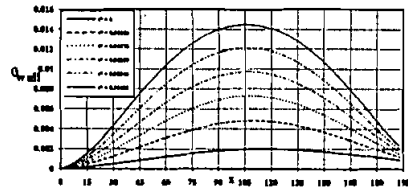
The steady state results of the previous section are used as the initial conditions for simulating the performance of the reactor core in the case of a sudden loss of coolant. Under such conditions, the problem reduces to that of unsteady conduction heat transfer in a thermally insulated heat-generating annulus. The temperature in the annulus is expected to increase with time, but at different rates; the temperatures in regions close to the coolant in steady state performance are expected to experience higher rates of increase than those nearer to the center of the annulus, especially since the walls are assumed to be insulated.

The above speculations are confirmed by the unsteady streamwise distribution of the wall (Figure 5b) and fuel centerline temperatures (Figure 5c) of the original nondiluted rod. The wall and fuel temperatures maintain the same shape with a shift in the maximum toward the center, where maximum heat generation occurs. This occurs because the rod is insulated, convection is totally lost, and the radial direction is the dominant direction of conduction heat transfer. From Figures 5b and 5c, it is obvious that the maximum wall temperature will reach its limiting value long before the fuel centerline temperature because it is increasing at a higher rate (e.g., at $t^* = 0.1$, $\theta_{w,max}$ increases by a factor of about 7, whereas $\theta_{fuel,max}$ increases by a factor of 2 only). Thus, attention should be directed toward maximizing the time delay before the maximum wall temperature reaches its limiting value.

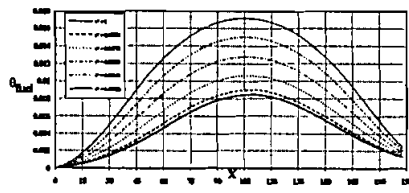
Maximum wall temperature. The variations of the maximum outer and inner wall temperatures with the amount of added diluent a (for $RC = 2$) are presented in Figures 6a–6d. Figures 6a and 6c show the temporal variation using dimensionless parameters, while Figures 6b and 6d show the same figures in dimensional form. As discussed earlier, increasing the amount of added diluent, represented by a , resulted in slight increase in the upper wall temperature during steady state performance. However, in the case of total loss of coolant, the factors affecting the temperature field are the geometry and the heat flux distribution. Increasing a results in lower radial temperature gradients due to the increase in diameter, so that lower wall and fuel temperatures are expected during transient



(a)



(b)



(c)

Figure 5. (a) Streamwise variation of inner and outer coolant bulk and wall temperatures for one-part and two-part dilutions. Transient axial distribution of (b) wall and (c) centerline temperatures in the original nondiluted rod.

performance. This is clearly shown in Figure 6b, where the time required for the maximum wall temperature to reach a certain value is seen to increase with increasing values of a . The curves in Figure 6b map into one curve when using dimensionless quantities (Figure 6a). This is because for a certain value of t^* the value of t depends on a . Similar improvements are noticed for the unsteady variations of maximum inner wall temperatures (Figure 6d). However, the curves in Figure 6d do not map into one curve in Figure 6c because t^* is based on d_o rather than on d_i , which remains constant ($RC = 2$) as a varies. Thus the transient performance shows improvement for both upper and lower wall temperatures, unlike the steady state performance for which only improvement in inner wall temperatures were obtained.

The temporal variations of maximum outer and inner wall temperatures with RC are presented using dimensional and dimensionless quantities in Figures 6e–6h. In contrast with the monotonic decrease in maximum wall temperature with increasing values of a , the curves in Figures 6f and 6h indicate the presence of an optimum RC value for which these temperatures are minimum (e.g., curves for $RC = 0.5$ are higher than those for $RC = 1$, which in turn, are lower than those for $RC = 3$). The wider spread in the curves when using dimensionless variables (Figures 6e and 6g) is due to a being constant.

As shown in Figure 6, improvements in time delay before melting of the fuel rod are of the order of a few seconds. These few seconds, however, are significantly

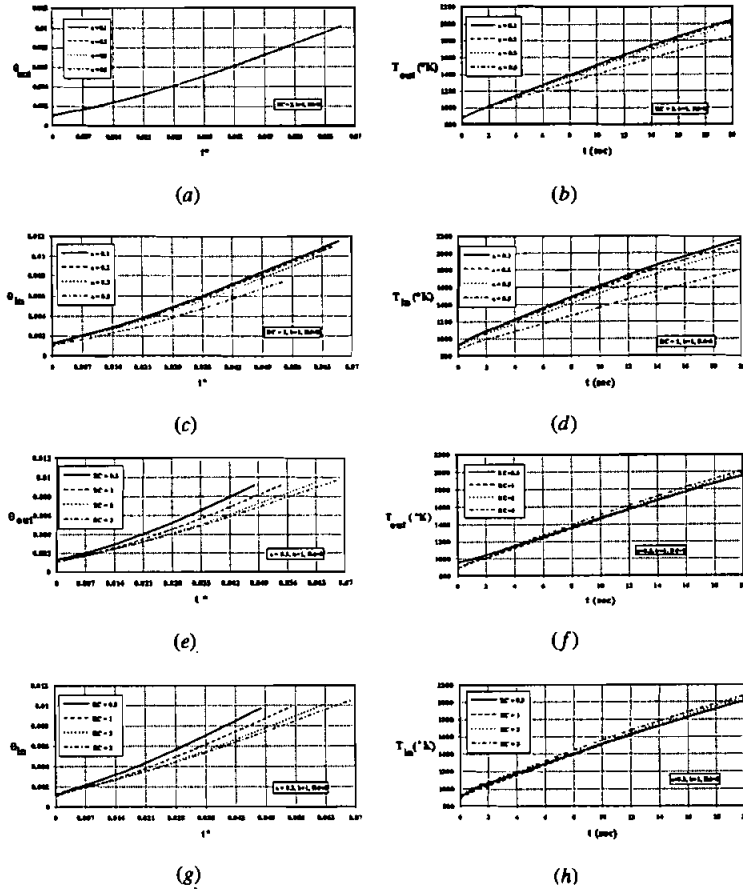


Figure 6. Variation of maximum dimensional and dimensionless outer and inner wall temperatures with time for various values of a and RC .

beneficial in an accident situation because in a typical gas-cooled reactor with prestressed pressure vessel, a depressurization usually takes place over a scale of minutes, with a typical exponential period in the neighborhood of 500 s [7]. The case studied in this work assumes a “worst case” situation, wherein the fuel (i.e., the fuel rod) becomes instantaneously isolated from the rod at the onset of depressurization. Therefore the additional few seconds in time delay obtained here will translate into an additional few minutes in an actual accident.

Maximum fuel temperature. In the steady state results section the variation of the maximum fuel temperature was not presented because, as already stated, the maximum wall temperature is the design temperature. However, for completeness of presentation, the variation of the maximum dimensionless fuel temperature with time for various values of a and RC are presented in Figures 7a–7d. As depicted, the trend of variation of the maximum fuel temperature is very

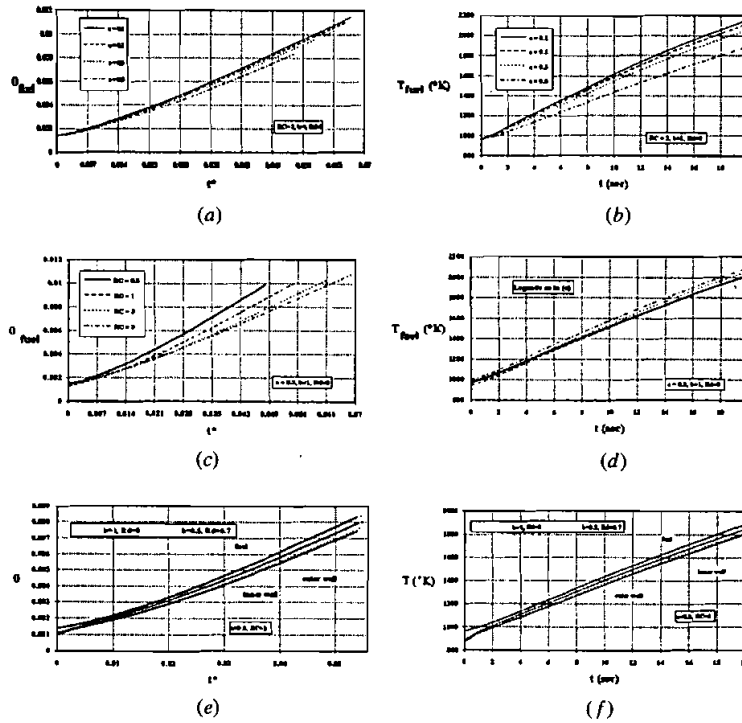


Figure 7. Variation of maximum (a, c) dimensionless and (b, d) dimensional fuel temperature with time for various values of (a, b) a and (c, d) RC. Variation of (e) dimensionless and (f) dimensional temperatures with time for one-part and two-part dilutions.

similar to that of the maximum wall temperature and will not be repeated. Furthermore, the results in Figures 7a–7d confirm that the maximum outer wall temperature reaches its limiting value long before the maximum fuel temperature.

The effects of diluent distribution using one-part and two-part dilution practices on the temporal variation of the maximum outer wall, inner wall, and fuel temperatures are shown comparatively in Figures 7e and 7f, respectively. Results indicate a mild influence of the diluent distribution on the thermal performance of the fuel rod.

CONCLUSION

The thermal performance under steady and unsteady conditions of radially diluted and centrally cooled nuclear fuel cells was investigated numerically. Results generated indicate a great reduction in the maximum wall temperatures of the fuel rod during steady operation and a noticeable increase in time delay before melting under unsteady conditions. In addition, results reveal the presence of an optimum RC value for which the maximum wall temperature is minimum. The method by which diluent is distributed proved to have little influence on the thermal perfor-

mance of the fuel rod. Most important, however, is the fact that lower wall temperature and longer time delay than those reported in Ref. [3] were obtained with less diluent addition. This somewhat alleviates the problem of retaining the "fast" mode of the reactor.

REFERENCES

1. M. A. Fischette, Inherently Safe Reactors: They'd Work if We'd Let Them, *IEEE Spectrum*, pp. 28–33, April 1987.
2. K. Hannerz and T. Pederson, PIUS—The Nuclear Reactor of Tomorrow, *Nucl. Eng.*, vol. 32, no. 5, pp. 162–171, 1991.
3. F. Moukalled, R. Y. Nuwayhid, and I. Lakkis, Transient Thermal Performance of Axially and Radially Diluted Nuclear Fuel Cells, *Numer. Heat Transfer* (in press).
4. A. E. Waltar and A. B. Reynolds, *Fast Breeder Reactors*, Pergamon, New York, 1981.
5. Weisman, J., *Elements of Nuclear Reactor Design*, Elsevier Scientific, Amsterdam, 1977.
6. Lamarsh, J. R., *Introduction to Nuclear Engineering*, Addison-Wesley, Reading, Mass., 1983.
7. W. B. Kemmish, Gas-Cooled Fast Reactors, *Nucl. Energy J. BNES*, vol. 21, no. 1, 1982.
8. Winterton, R. H. S., *Thermal Design of Nuclear Reactors*, Pergamon, New York, 1981.
9. H. Schlichting, *Boundary Layer Theory*, 7th ed., pp. 475–531, McGraw-Hill, New York, 1960.
10. F. Moukalled, J. Kasamani, and S. Acharya, Turbulent Convection Heat Transfer in Longitudinally Conducting Externally Finned Pipes, *Numer. Heat Transfer Part A*, vol. 21, pp. 401–421, 1992.
11. J. Nikuradse, Gesetzmässigkeit der turbulenten Stromung in glatten Rohren, *Forschungshet*, p. 356, 1932.
12. E. R. Van Driest, On Turbulent Flow near a Wall, *J. Aerosol Sci.*, vol. 23, pp. 1007–1011, 1956.
13. S. V. Patankar and D. B. Spalding, *Heat and Mass Transfer in Boundary Layers*, Intertext Books, London, 1970.
14. S. V. Patankar, *Numerical Heat Transfer and Fluid Flow*, Hemisphere, New York, 1980.